CI2 – Inviscid Strong Vortex-Shock Wave Interaction


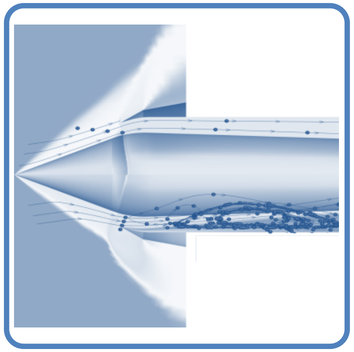
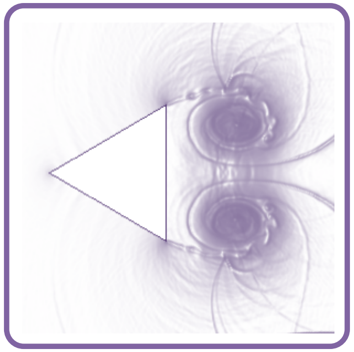

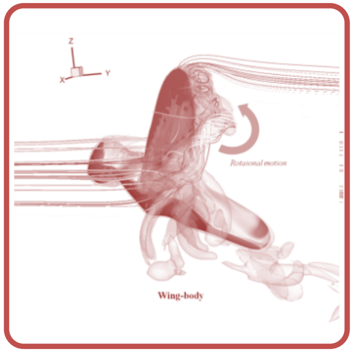

Chongam Kim

(with Hojun You, Seonghun Cho)

Department of Mechanical and Aerospace Engineering

Seoul National University, Korea

Jan. 6-7, 2018

Introduction

Problem Description

- **Test objective**
  - **Capability of capturing unsteady compressible flow physics qualitatively**
    - Post-shock vortical structure due to compression effects
    - Propagation of discontinuous waves and cylindrical acoustic waves
  - **Attempts to evaluate unsteady flow solution quantitatively**
    - Quantification of monotonicity across shock
    - Quantification of discrete shock-driven numerical oscillations
    - Evaluation of error and order-of-accuracy in post-shock region

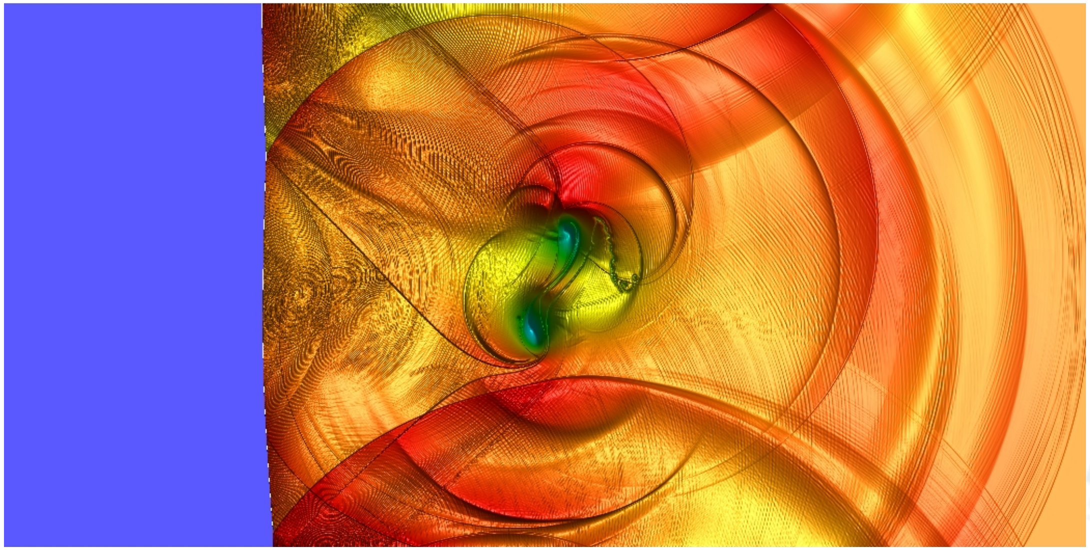

CI2 – Density Contour of Reference Solution

Problem Description

- **Initial condition**
  - **Non-dimensional 2-D Euler equations with EOS for ideal gas**
  - **Initially, the flow field contains a stationary shock and a strong vortex located in upstream.**
  - **Composite vortex with C^0-continuous angular velocity and C^1-continuous density profiles**

$$\frac{v_\theta}{v_m} = \begin{cases} \dfrac{r}{a} & \text{if } r \le \mathrm{a}, \\ \dfrac{a}{a^2 - b^2}\left(r - \dfrac{b^2}{r}\right) & \text{if } \mathrm{a} < r \le \mathrm{b}, \\ 0 & \text{if } r > \mathrm{b}. \end{cases}$$

※ $(a, b) = (0.075,\ 0.175)$

  - $M_v = v_m/\sqrt{\gamma}$ **as a measure of the vortex strength**

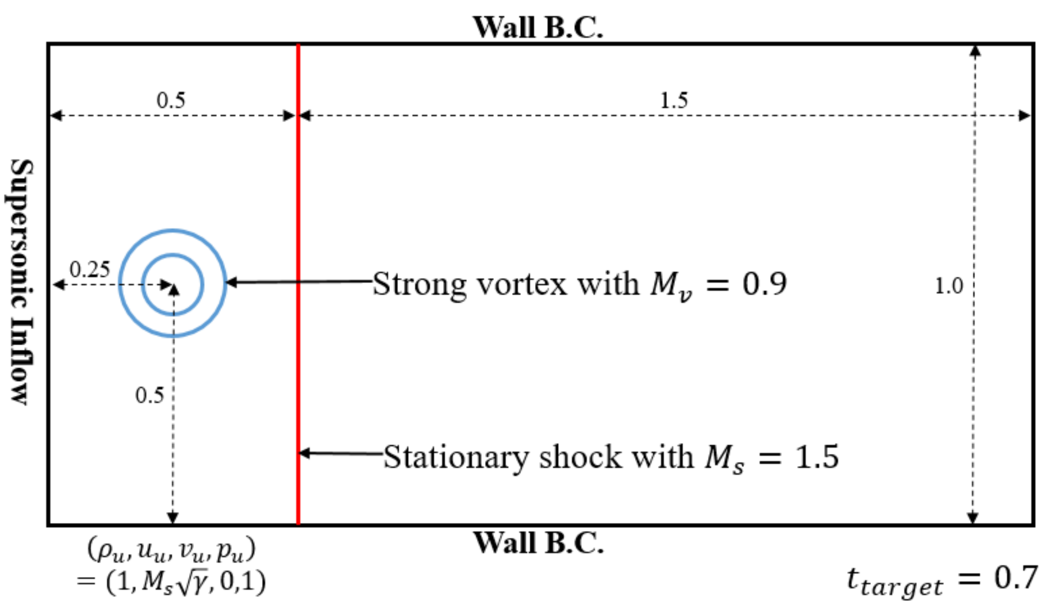

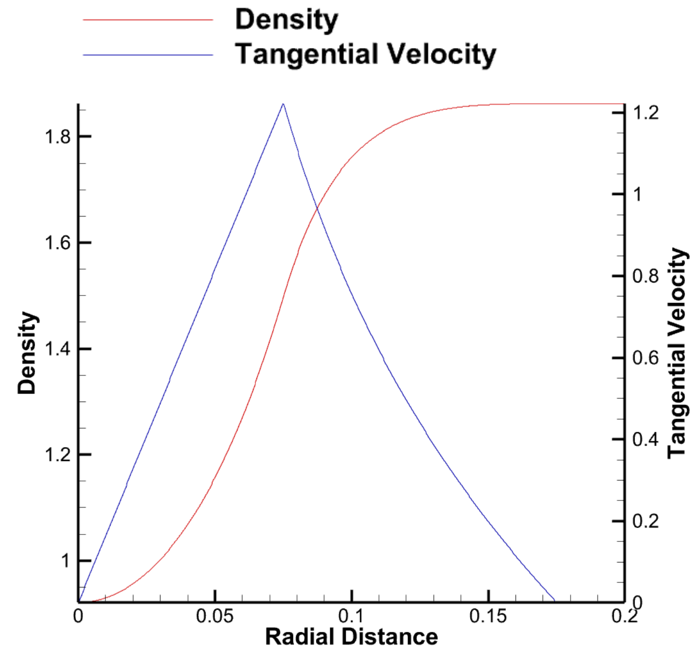

Composite Vortex Model

Problem Description

- **Grid definition**
  - **Rule of mesh naming: Abbreviation of mesh type-Reciprocal of mesh size**
    - Ex) RT50, RQ100, etc.

Mesh type	Abbreviation	Reciprocal of mesh size, $\frac{1}{h}$
Regular Triangle	RT	50, 100, 150, 200, 250, 300
Irregular Triangle	IT	50, 100, 150, 200, 250, 300
Regular Quadrilateral	RQ	50, 100, 150, 200, 250, 300
Mixed	M	50, 100, 150, 200, 250, 300

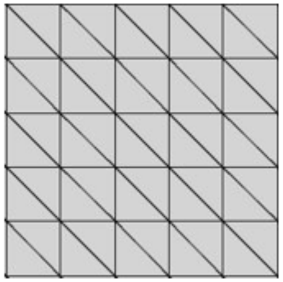
[RT type]

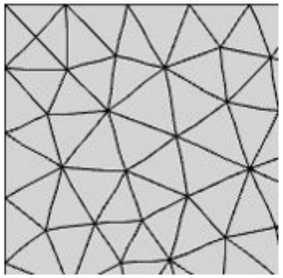
[IT type]

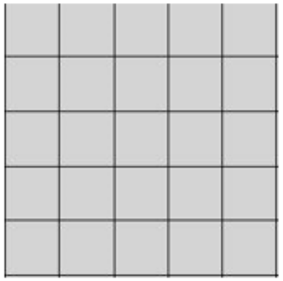
[RQ type]

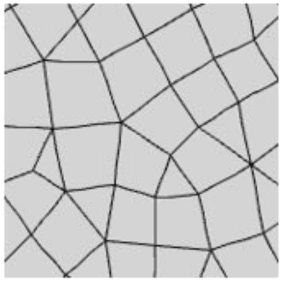
[M type]

Problem Description

- **Flow field description**

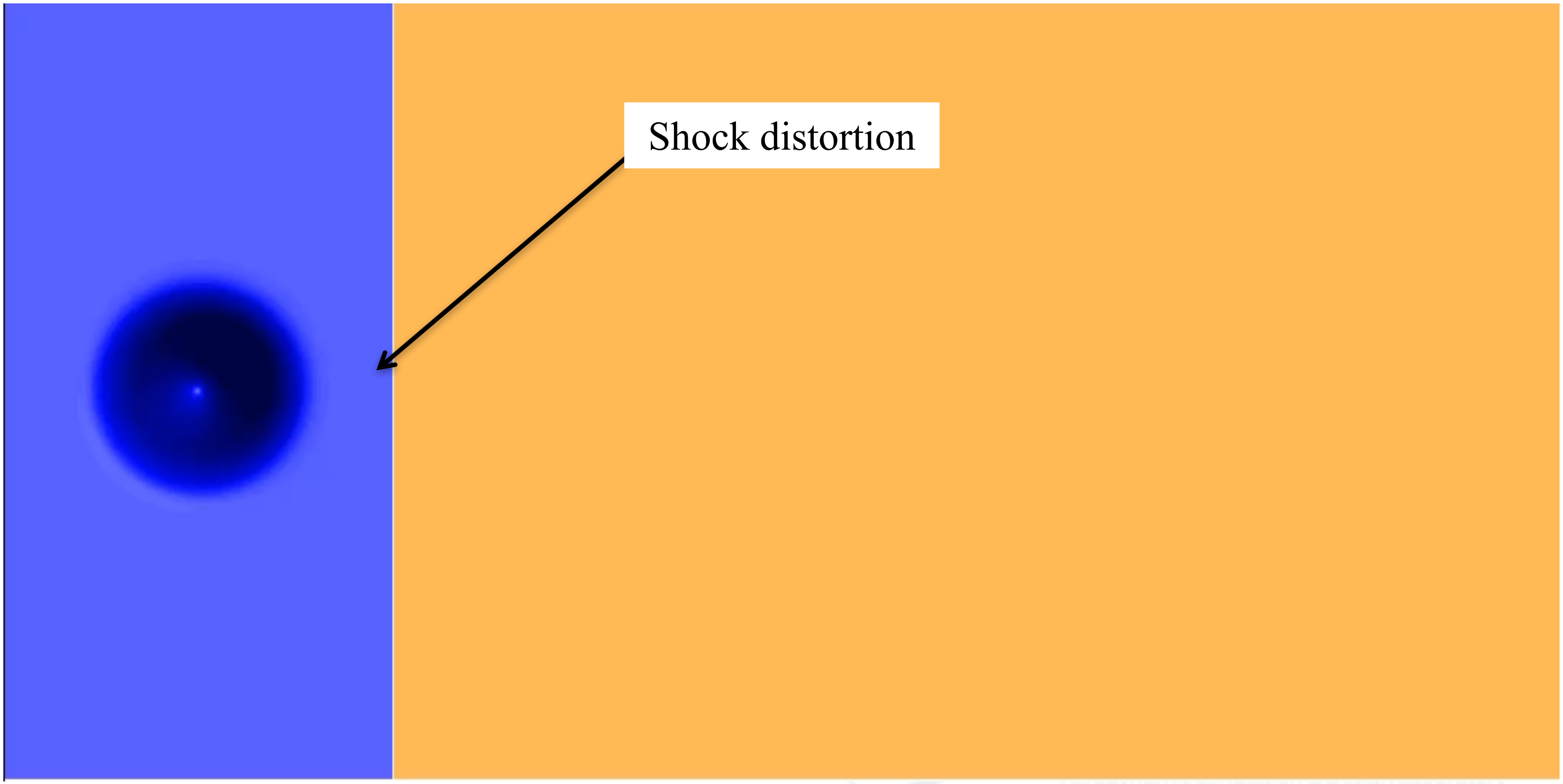

Problem Description

- **Flow field description**

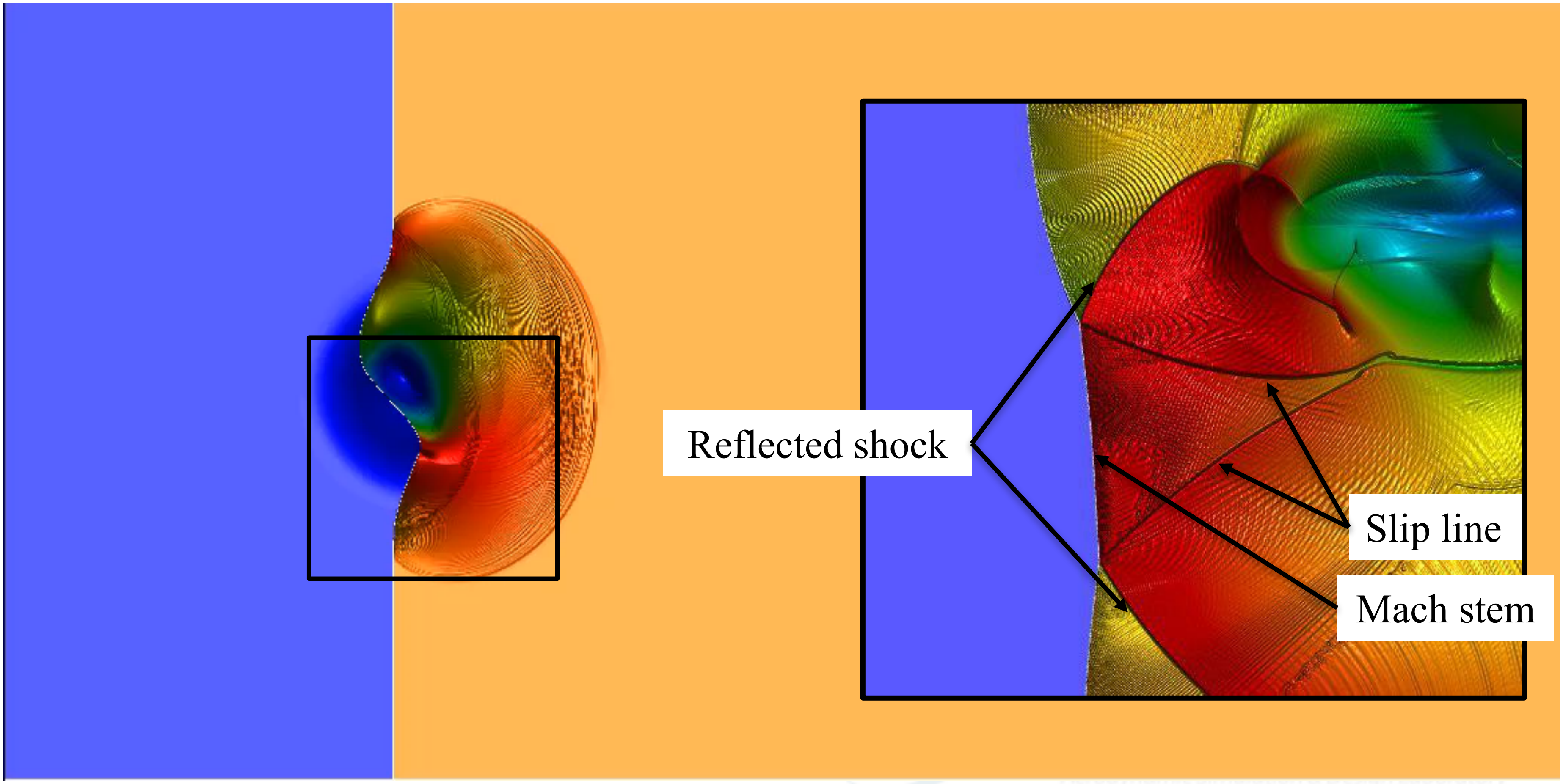

- **Flow field description**

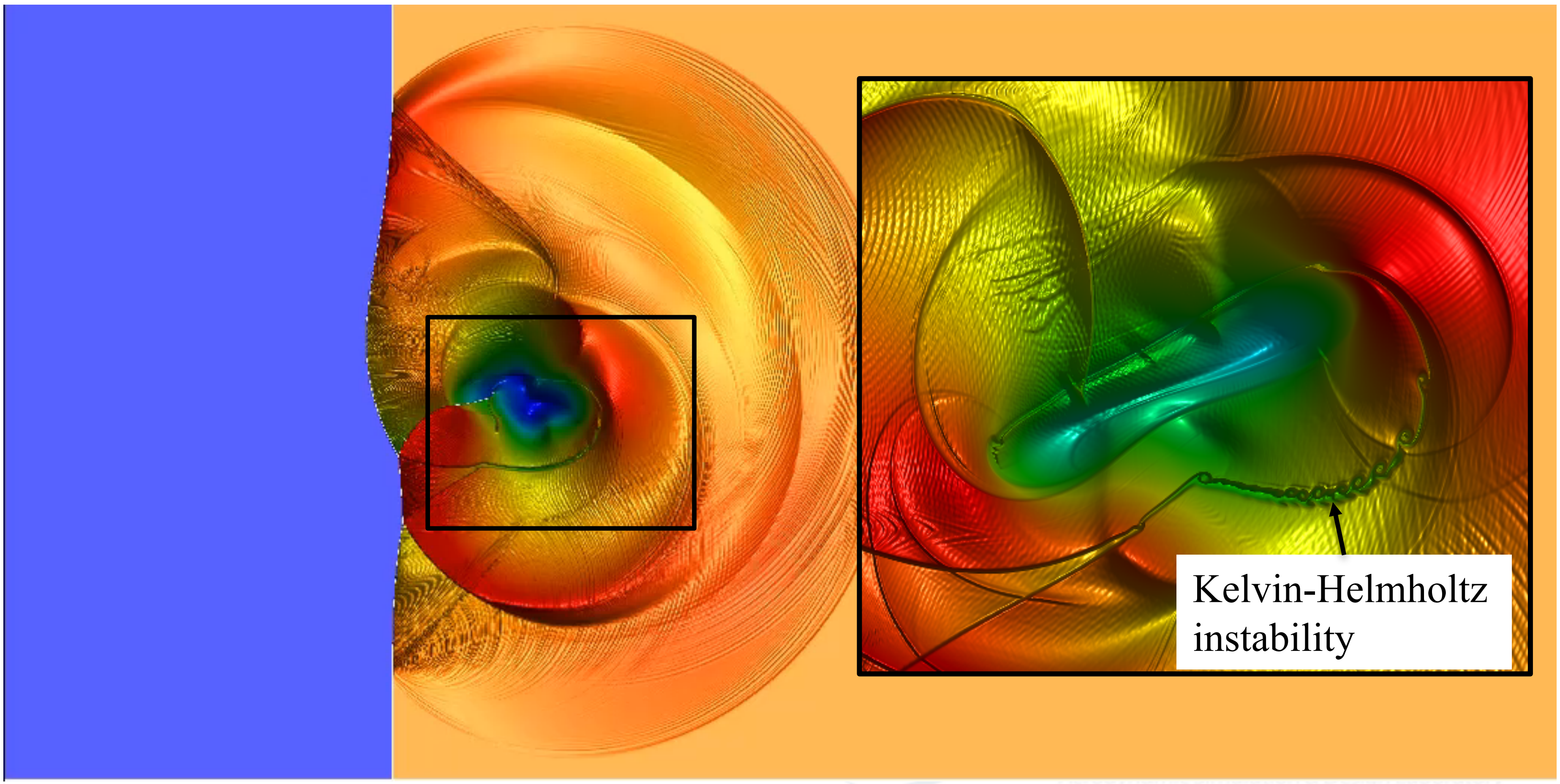

Problem Description

- **Flow field description**

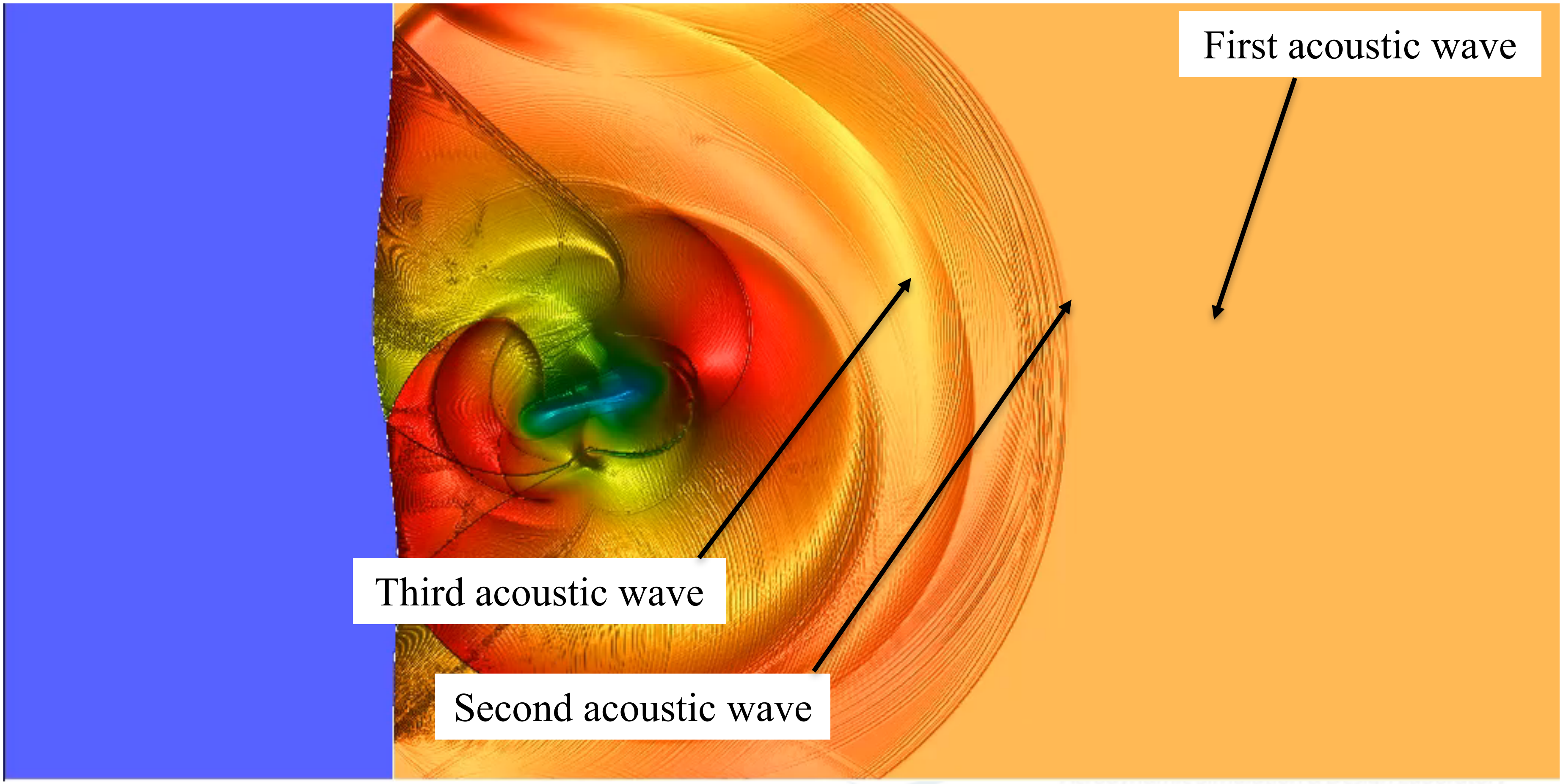

Problem Description

- **Flow field description**

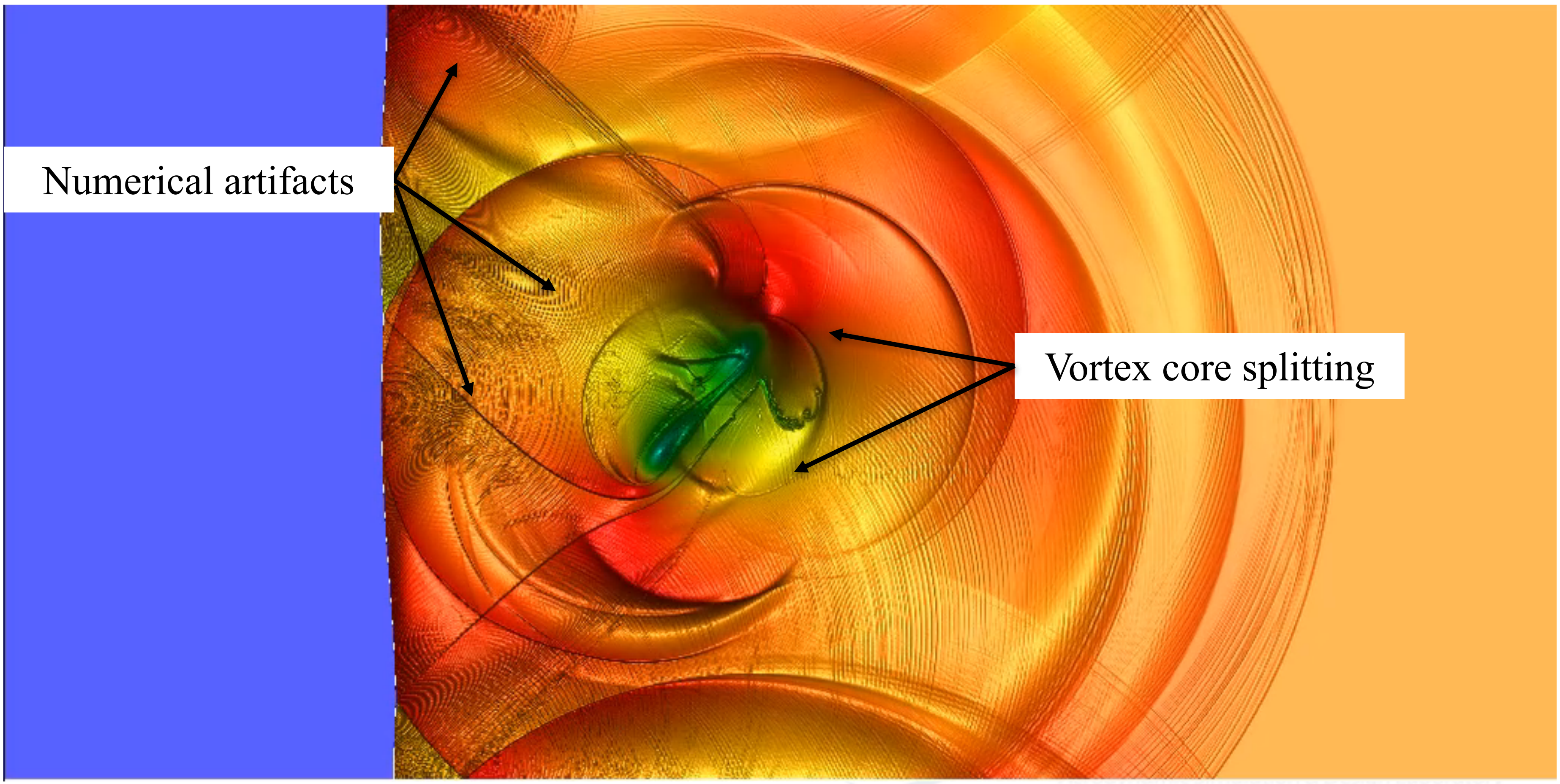

Problem Description

- **Reference lines for data submission**

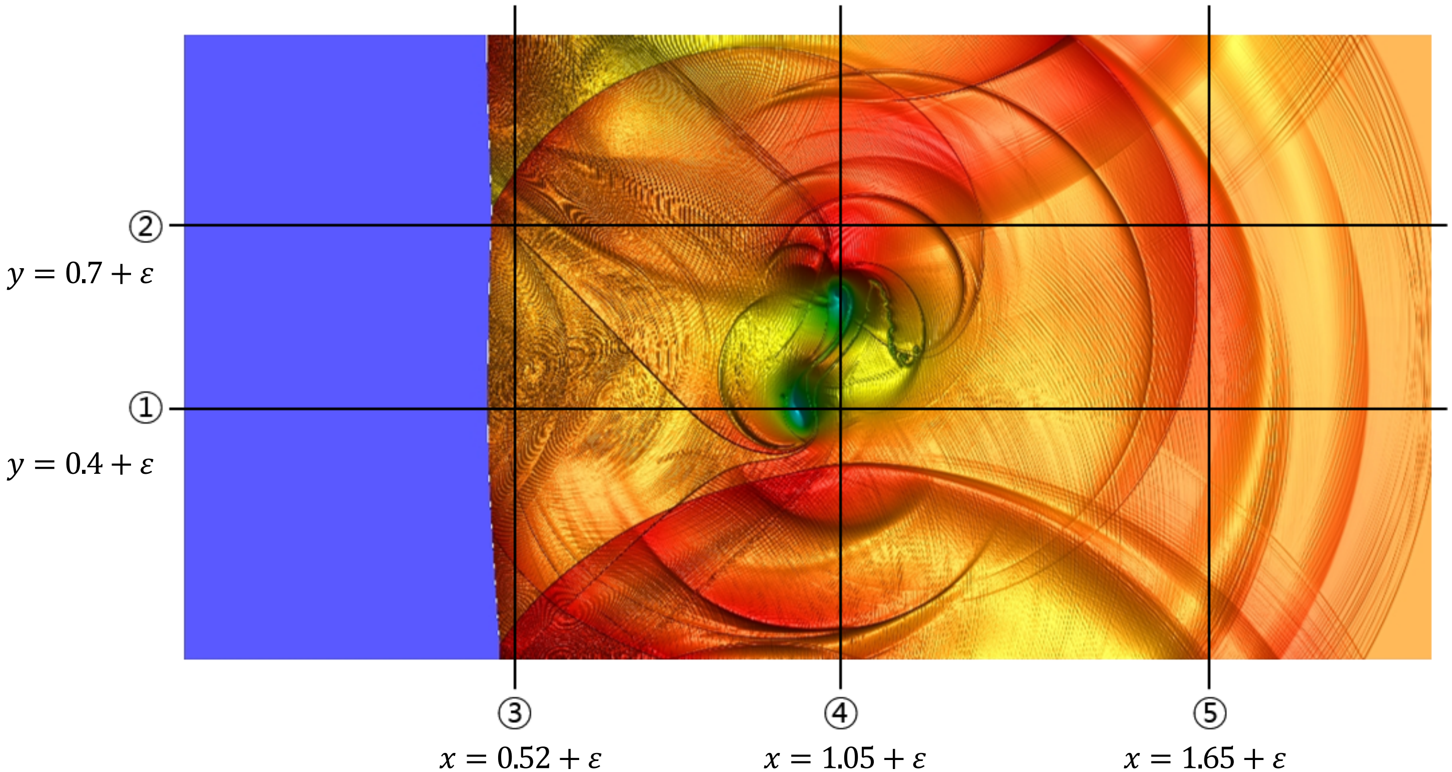

Num.	①	②	③	④	⑤
Physical meaning	Stationary shock & vortex center	Stationary shock	Right after stationary shock	Vortex center	Far downstream

※ $\varepsilon = 1\times10^{-4}$ is to avoid the cell interfaces.

Reference Solution

- **Setting the reference solution**
  - **Reference solution is computed by FVM on extremely fine meshes.**
    - Ref1000: Number of cells = 2,700,000 / $h_{min} = 1/2000$
    - Ref2000: Number of cells = 10,800,000 / $h_{min} = 1/4000$
    - Ref3000: Number of cells = 24,300,000 / $h_{min} = 1/6000$

    ⇒ The result with Ref3000 mesh is adopted as the reference solution.
    - FVM solver with Roe flux / 3rd-order TVD-RK for spatial- / temporal-discretization, and MLP5 limiter for shock-capturing

Ref3000 Mesh

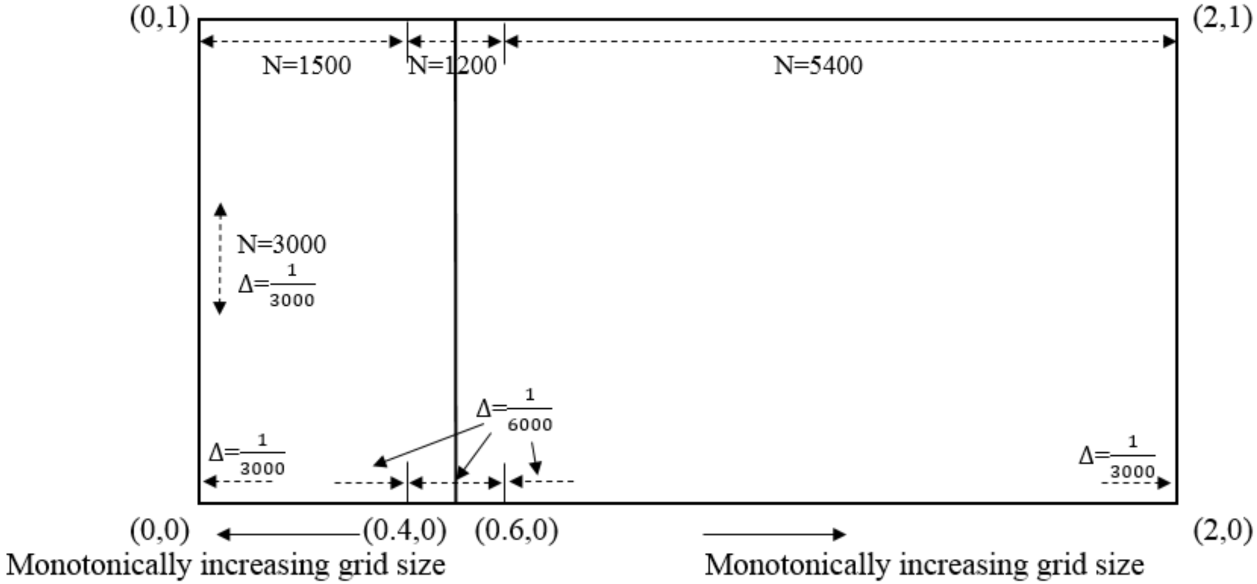

Reference Solution

- **Removal of non-physical oscillations with filtering technique**
  - **Low-pass filter is applied to some reference lines.**
    - Gaussian filtering is applied to Line 1~3 where non-physical oscillations/noises occur noticeably.
      - Filtering is locally applied by considering the amplitude of local non-physical oscillations.
      - Cut-off frequency where the response value becomes $\exp(-0.5) \approx 0.607$ is locally determined as 3~5 times of noticeable oscillatory frequency from FFT results.
      - Saturation phenomenon is not observed during grid refinement test using the filtered reference solution.
    - Conservation laws are still satisfied when the low-pass filter is applied.

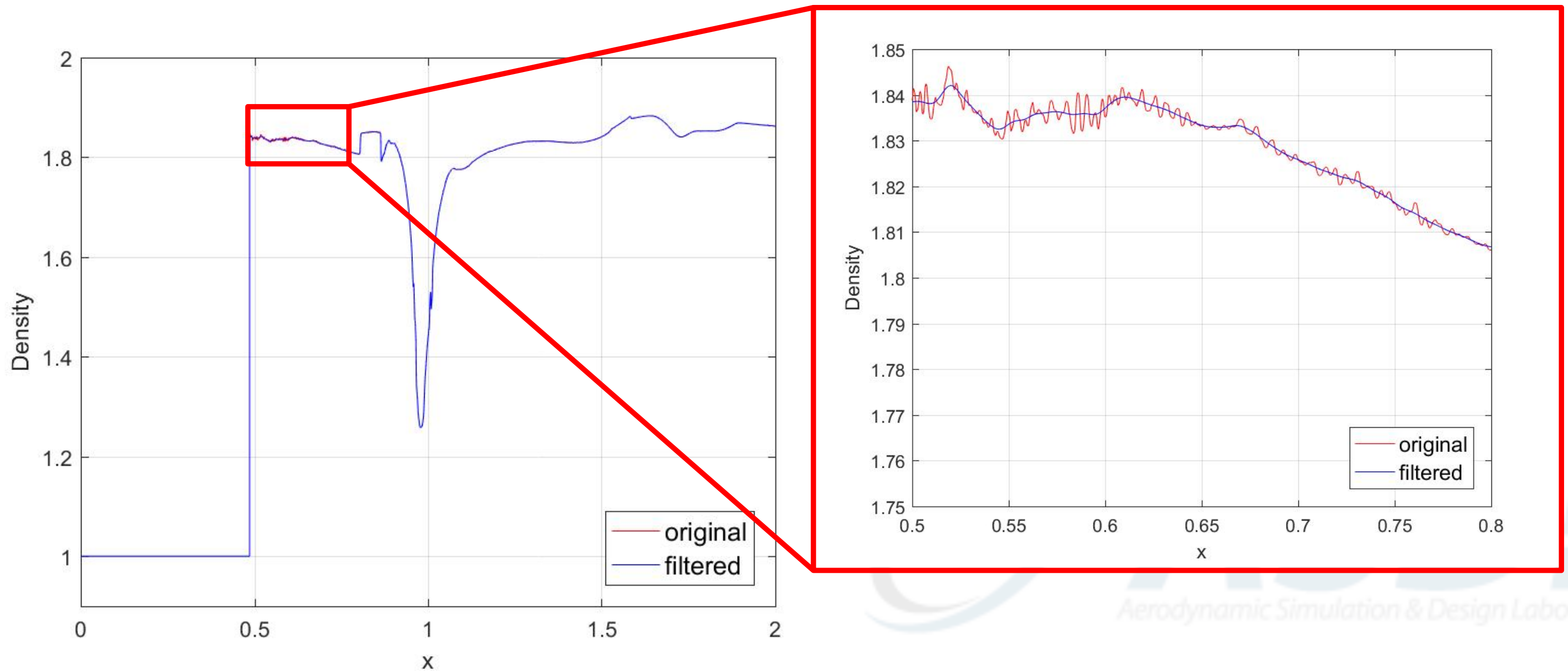

Density Distribution along Line 1

Verification Test (VI1 – Inviscid Convected Vortex)

- **Inviscid isentropic Taylor vortex is transported by uniform flow for 50 periods.**

$$u_0 = U_\infty\left(1 - \beta\frac{y - Y_c}{R}e^{-r^2/2}\right) \qquad T_0 = T_\infty - 0.5(\beta U_\infty e^{-r^2/2})^2/C_p$$

$$v_0 = U_\infty\beta\frac{x - X_c}{R}e^{-r^2/2} \qquad \rho_0 = \rho_\infty(T_0/T_\infty)^{1/(\gamma-1)}$$

- **Two types of freestream conditions**
  - Slow: Mach number = 0.05
  - Fast: Mach number = 0.5
- **Results**
  - L2-norm error vs. Length scale
  - L2-norm error vs. Time unit
- **Four types of meshes**
  - Regular triangle
  - Regular quadrilateral
  - Randomly perturbed regular triangle
  - Randomly perturbed regular quadrilateral

Participants

- **University of Kansas**
  - **FR/CPR method[1] with $P2$ and $P3$ approximations**
  - **Explicit TVD-RK3**
  - **SMOOTH limiter[2]**
  - **Roe solver**

- **University of Michigan**
  - **DG method with $P1$ and $P3$ approximations**
  - **Explicit RK4 for CI2 and VI1-$P1$ / Explicit 8th-order 13-stage RK for VI1-$P3$**
  - **PDE-based artificial dissipation method[3] (with BR2 method)**
  - **SLAU2 Riemann solver[4] on RQ-$P1$ / Roe solver for the others**
  - **ICB-N method[5] for recovery on RQ**

- **Seoul National University**
  - **DG method with $P1$, $P2$ and $P3$ approximations**
  - **Explicit TVD-RK3 for $P1$ and $P2$ / Explicit 4th-order 5-stage SSP-RK for $P3$**
  - **hMLP[6] and hMLP_BD limiter[7] (tagged as SNU1 and SNU2 in the following figures)**
  - **Local Lax-Friedrich flux for VI1 / Roe solver for CI2**

Participants

- **University of Kansas**
  - **VI1**
    - Total 20 (Slow vortex) cases
      - No limiter and SMOOTH limiter
      - $P2$ and $P3$ approximations on RQ meshes with $1/h$ = 16, 32, 64, 128, 256
  - **CI2**
    - Total 12 cases
      - SMOOTH limiter
      - $P2$ and $P3$ approximations on RQ meshes with $1/h$ = 50, 100, 150, 200, 250, 300
- **University of Michigan**
  - **VI1**
    - Total 28 (Slow vortex) + 32 (Fast vortex) cases
      - PDE-based artificial dissipation
      - $P1$ and $P3$ approximations on RQ, RT, rpRQ and rpRT meshes with $1/h$ = 16, 32, 64, 128, 256
  - **CI2**
    - Total 18 cases
      - PDE-based artificial dissipation
      - $P1$ and $P3$ approximations on IT and RQ meshes with $1/h$ = 50, 100, 150, 200, 250, 300
- **Seoul National University**
  - **VI1**
    - Total 76 (Slow vortex) + 81 (Fast vortex) cases
      - No limiter, hMLP and hMLP_BD limiters
      - $P1$, $P2$ and $P3$ approximations on RQ and RT meshes with 1/h = 16, 32, 64, 128, 256
  - **CI2**
    - Total 96 cases
      - hMLP and hMLP_BD limiters
      - $P2$ and $P3$ approximations on RT, IT, RQ and M meshes with 1/h = 50, 100, 150, 200, 250, 300

References

[1] Z. J. Wang and H. Gao. "A unifying lifting collocation penalty formulation including the discontinuous Galerkin, spectral volume/difference methods for conservation laws on mixed grids." *Journal of Computational Physics* 228.21 (2009): 8161-8186.

[2] Y. Li and Z. J. Wang. "A convergent and accuracy preserving limiter for the FR/CPR method." *55th AIAA Aerospace Sciences Meeting*. 2017.

[3] J. Reisner, J. Serencsa and S. Shkoller. "A space–time smooth artificial viscosity method for nonlinear conservation laws." *Journal of Computational Physics* 235 (2013): 912-933.

[4] K. Kitamura and E. Shima. "Towards shock-stable and accurate hypersonic heating computations: A new pressure flux for AUSM-family schemes." *Journal of Computational Physics* 245 (2013): 62-83.

[5] P. Johnson, To be presented at 2018 SciTech meeting.

[6] J. S. Park and C. Kim. "Higher-order multi-dimensional limiting strategy for discontinuous Galerkin methods in compressible inviscid and viscous flows." *Computers & Fluids* 96 (2014): 377-396.

[7] H. You and C. Kim. "Higher-Order Multi-Dimensional Limiting Strategy for Subcell Resolution." *23rd AIAA Computational Fluid Dynamics Conference*. 2017.

Summary

Verification Test (VI1 – Inviscid Convected Vortex)

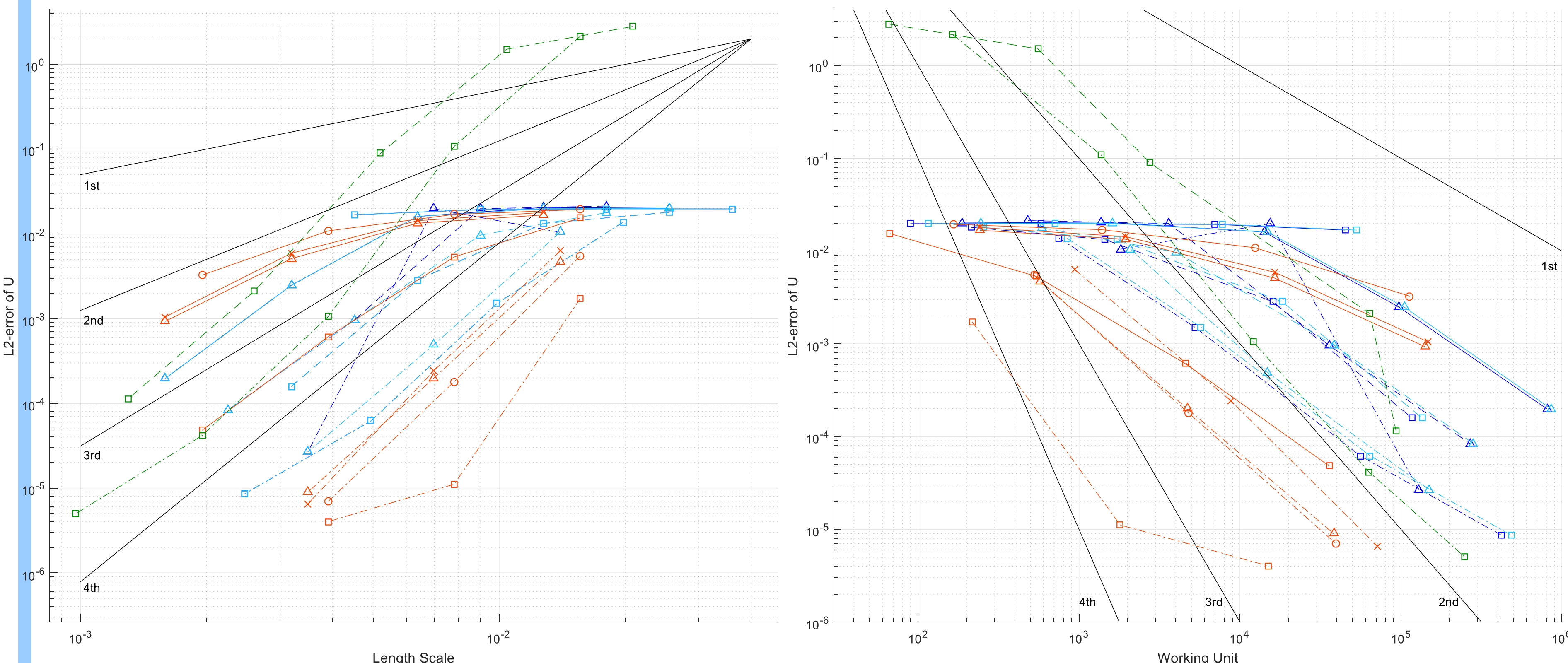

Slow Vortex ($M = 0.05$)

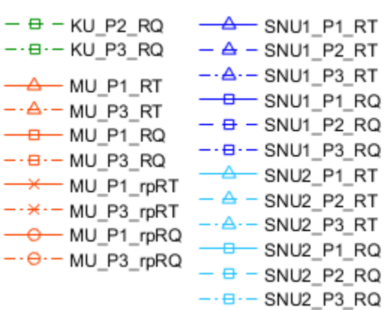

Verification Test (VI1 – Inviscid Convected Vortex)

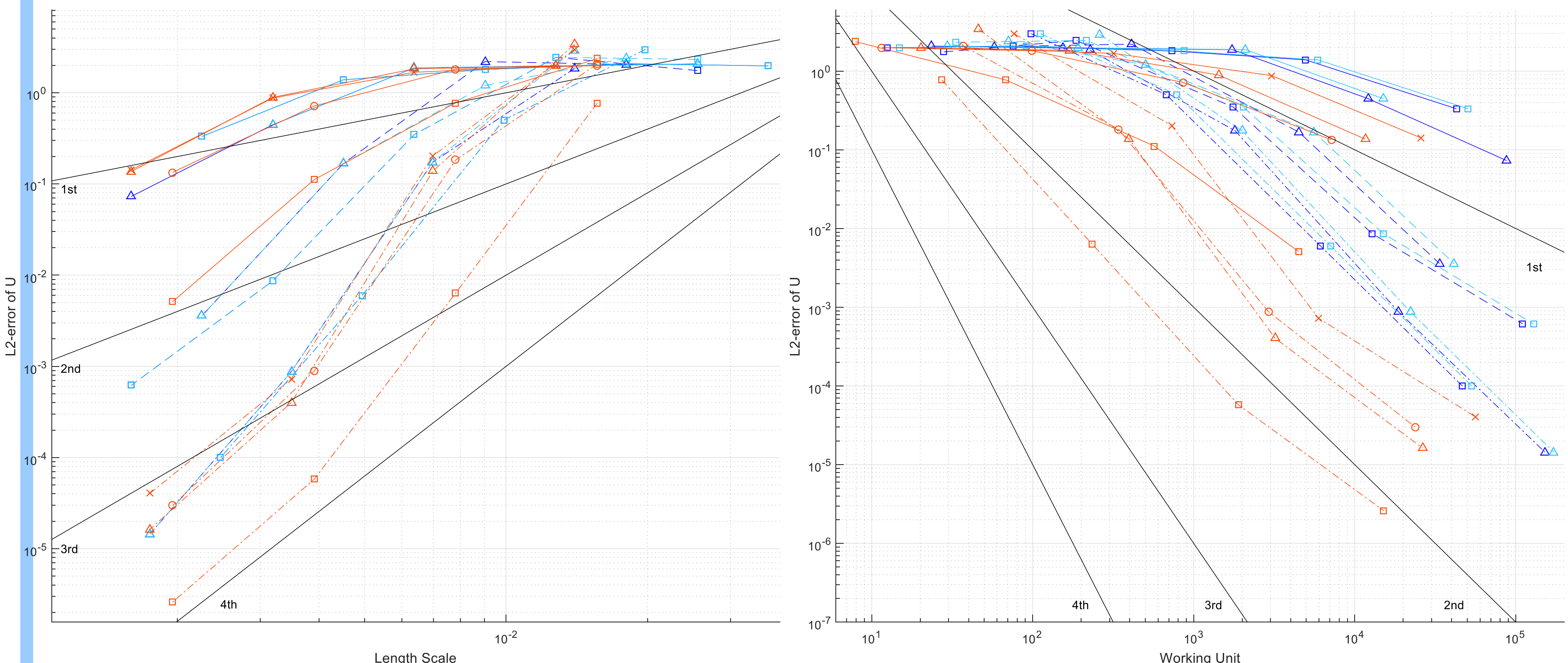

Fast Vortex ($M = 0.5$)

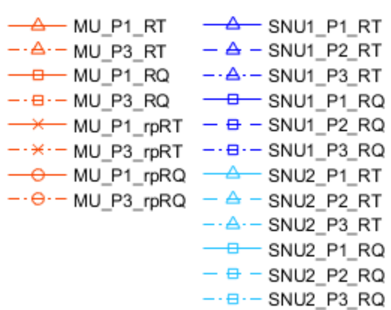

Results (Schlieren View)

- **Effects of numerical schemes**

Reference

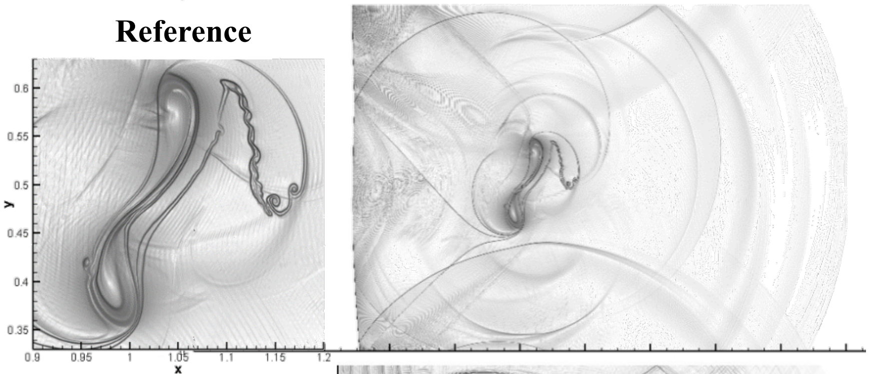

KU_P3_RQ300

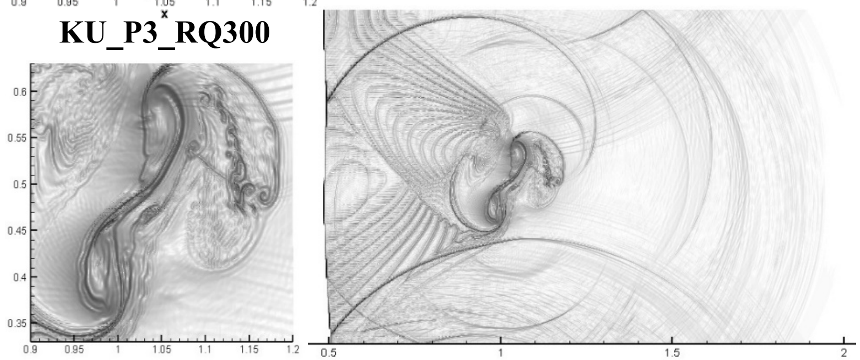

MU_P3_RQ300

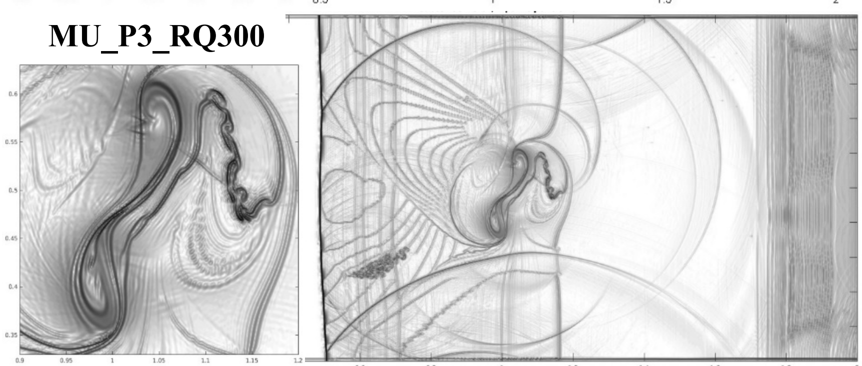

- **Well-resolved flow structures with much less DOFs**
  - Vortex core splitting
  - Complex shock structure
  - Kelvin-Helmholtz instability along slip layer
- **Undesirable numerical artifacts**
  - Shock-driven oscillations
  - Small scale wiggles
  - Spurious wave structures

SNU1_P3_RQ300

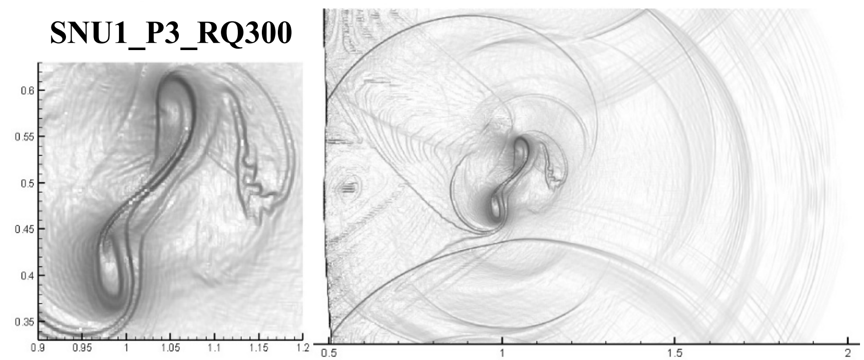

SNU2_P3_RQ300

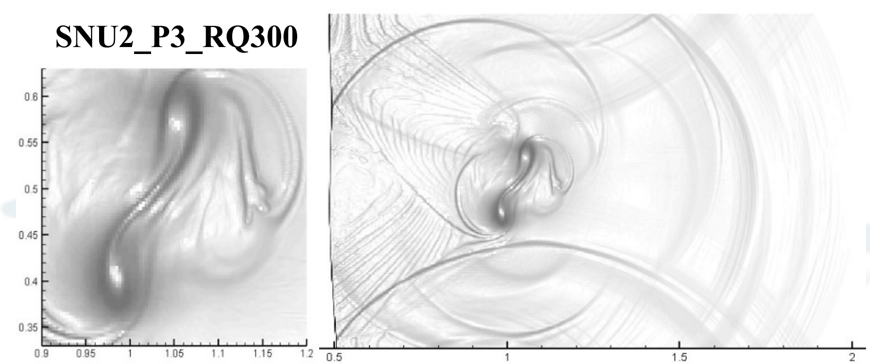

Results (Schlieren View)

- **Effects of mesh types**

Reference

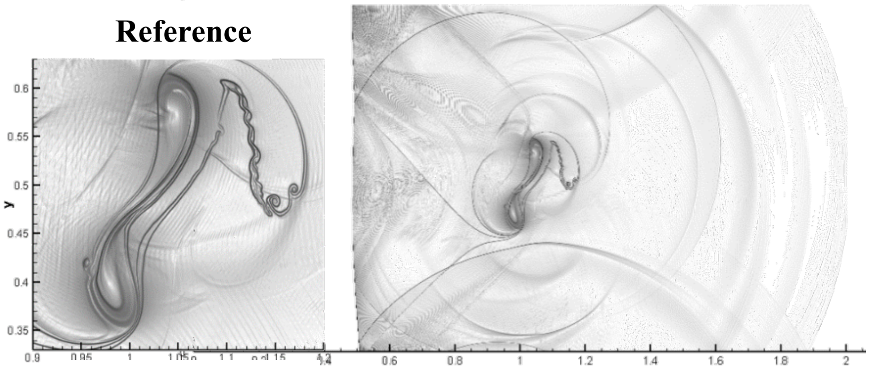

- **Large scale flow structure is still captured.**
  - Higher resolution with IT meshes results from the increase of DOF.
- **Mesh type dependence of numerical artifacts**
  - Shock-driven oscillation patterns

MU_P1_RQ300

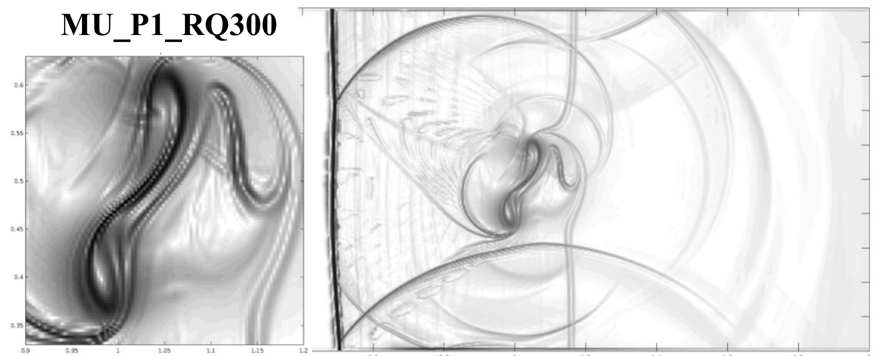

MU_P1_IT300

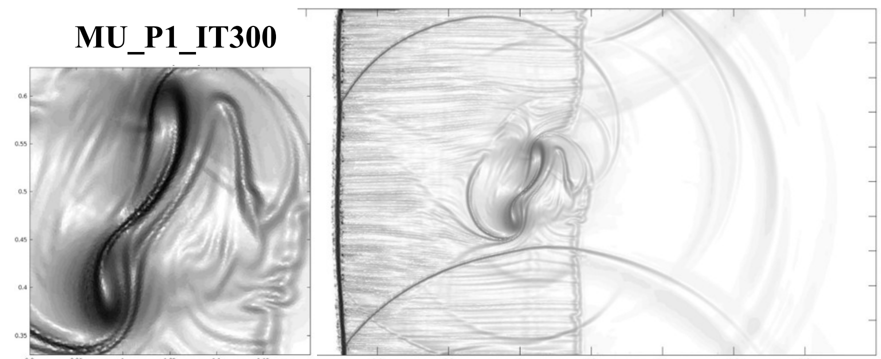

SNU2_P3_RQ300

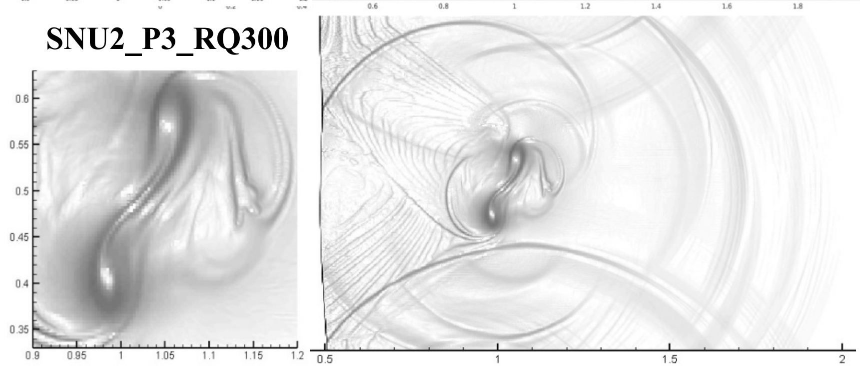

SNU2_P3_IT300

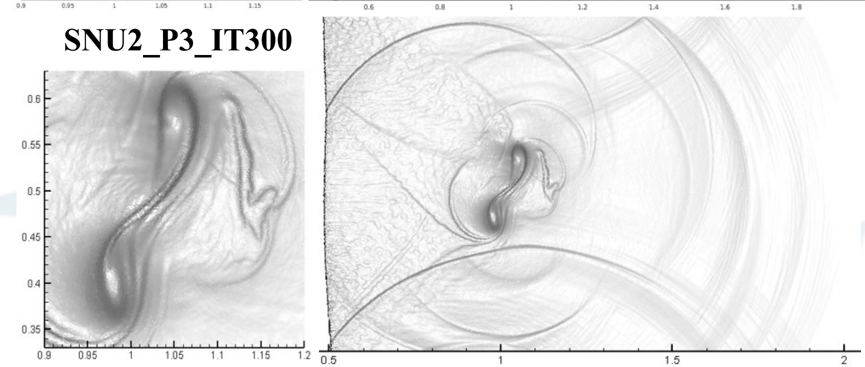

Results (Line 1)

- **Well-resolved large scale flow structure along Line 1**
  - **Shock and vortex core are captured.**
  - **Numerical artifacts around the shock and outflow region are clearly shown.**
- **Solution behavior around vortex core**
  - **Location and depth of the vortex core are different with various schemes.**
  - **Some schemes show numerical artifacts that are different from the reference solution.**

Line 1 (RQ250)

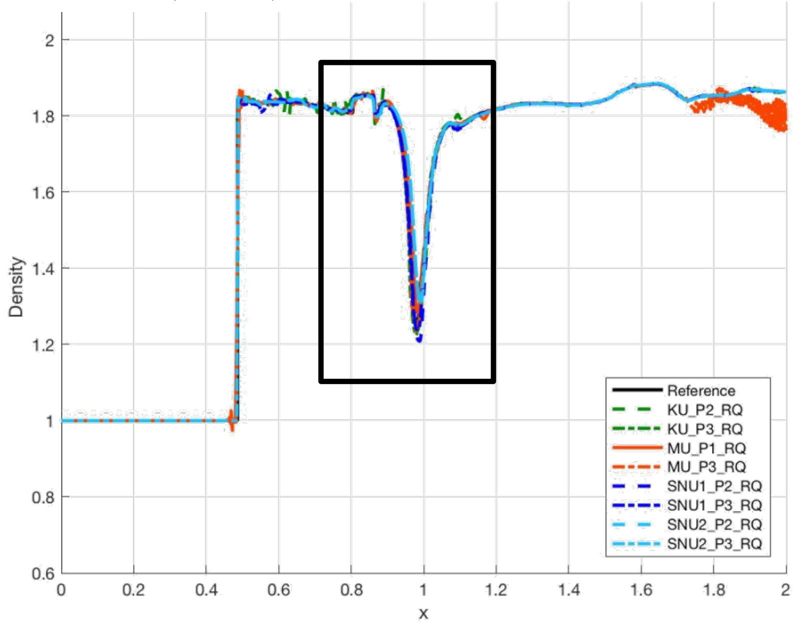

Line 1 (Vortex Core Close-up)

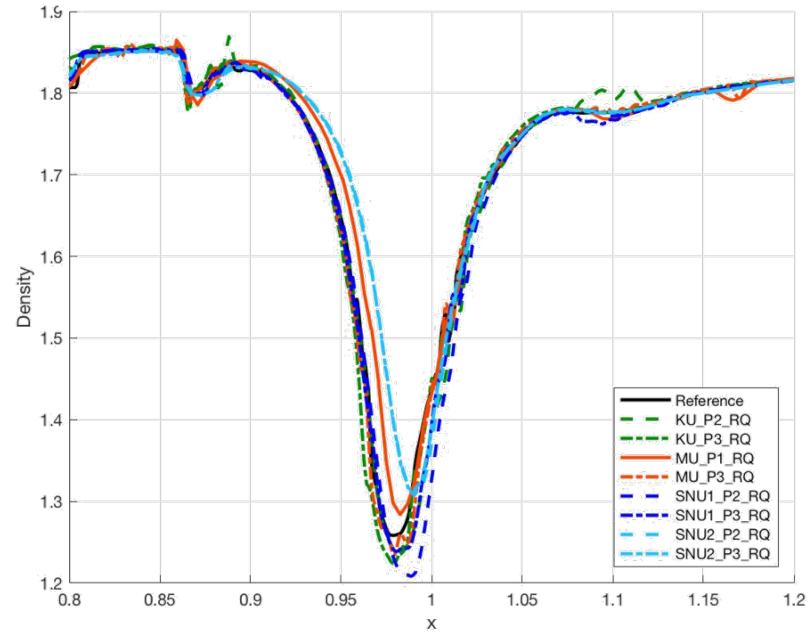

Results (Line 1)

- **Solution behavior around the stationary shock**
  - **Shock thickness is different with various schemes.**
  - **Monotonicity of the shock may not be satisfied.**
- **Evaluation of shock monotonicity**
  - **Total variation and maximum undershoot normalized by the shock strength on the region containing the shock, $0.47 < x < 0.5$.**
  - **Non-monotonic shock profile shows either large total variation or large maximum undershoot.**

Line 1 (Shock Close-up)

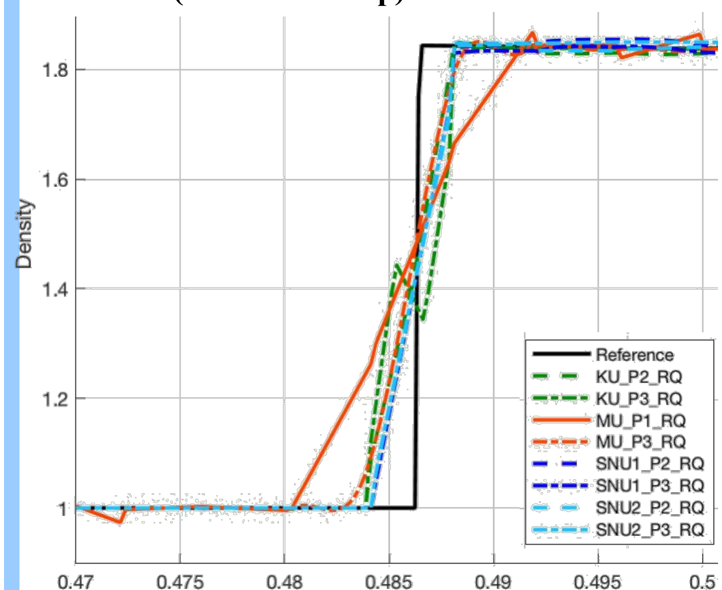

Comparison of Monotonicity across Shock (*P*3 on RQ meshes)

		KU	MU	SNU1	SNU2
RQ150	Total Variation*	1.069	1.452	1.099	0.9942
	Max Undershoot*	2.069E-2	1.189E-2	7.077E-3	3.460E-7
RQ250	Total Variation*	1.212	1.177	0.9995	1.000
	Max Undershoot*	1.370E-8	4.939E-3	4.082E-11	1.254E-7

***: Normalized by the shock strength ($\Delta\rho \approx 8.620\times10^{-1}$)**

Results (Line 1)

- **Computation of error and order-of-accuracy along Line 1**
  - **Post-shock region ($x \geq 0.9$) is considered to compute errors with the filtered reference solution.**
  - **Order-of-accuracy is degraded from formal $(n+1)^{th}$-order accuracy for Pn approximation.**
    - All schemes show approximately ~ 2nd ~ -order accuracy.
  - **Computed errors show slower change in coarser meshes and tend to decrease faster in finer meshes.**
    - Grid size may act as a threshold of numerical error.

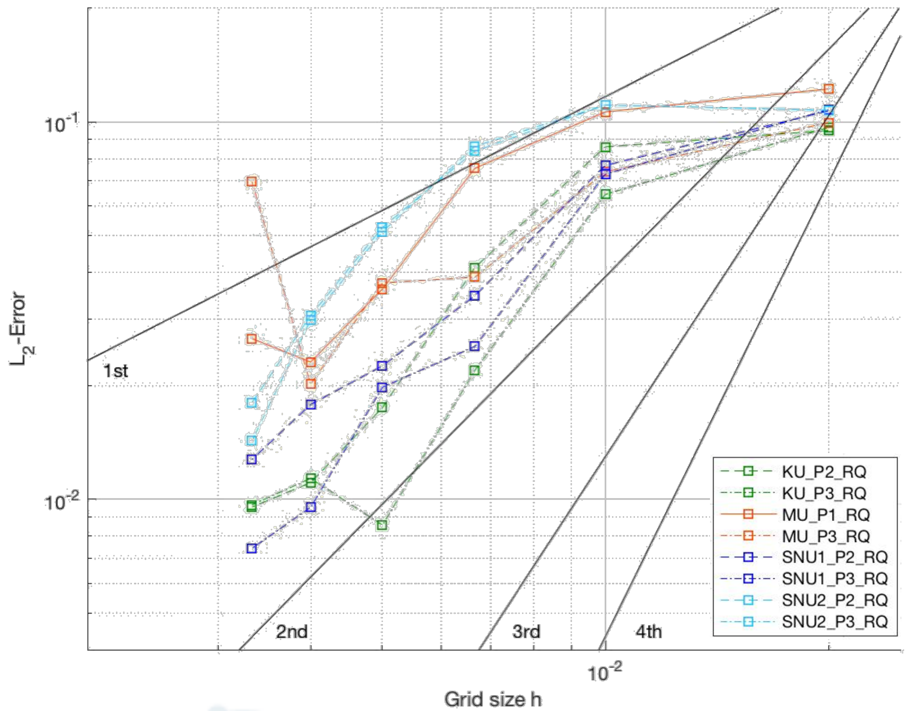

Grid Refinement Tests along Line 1 in Post-shock Region

Results (Line 3)

- **Evaluation of shock-driven oscillations**
  - **Shock-driven oscillations are clearly shown regardless of the discretization schemes.**
  - **Total variation and maximum difference with respect to the filtered reference solution on the domain of $0.2 < y < 0.6$.**
  - **Severe shock-driven oscillations result in larger total variation and maximum difference than the filtered reference solution.**

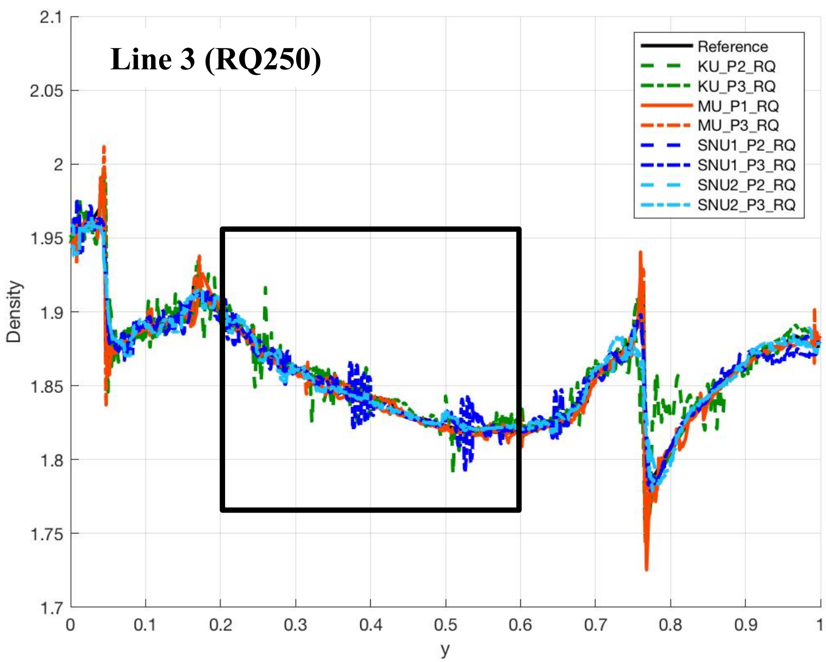

Comparison of Oscillations (*P*3 on RQ250 meshes)

	KU	MU	SNU1	SNU2
Total Variation*	5.939E-1	3.765E-1	9.598E-1	2.281E-1
Max Difference	1.289E-2	1.228E-2	2.938E-2	1.074E-2

***: Reference total variation = 8.270E-2**

- **Solution behavior on the downstream region**
  - **Shock-driven oscillations far downstream are rather damped out.**
  - **Similar to Line 1, computed order-of-accuracy is degraded to ~ 2^{nd} ~ -order accuracy for most of the schemes.**
  - **Computed error does not show threshold-like behavior on coarse mesh.**

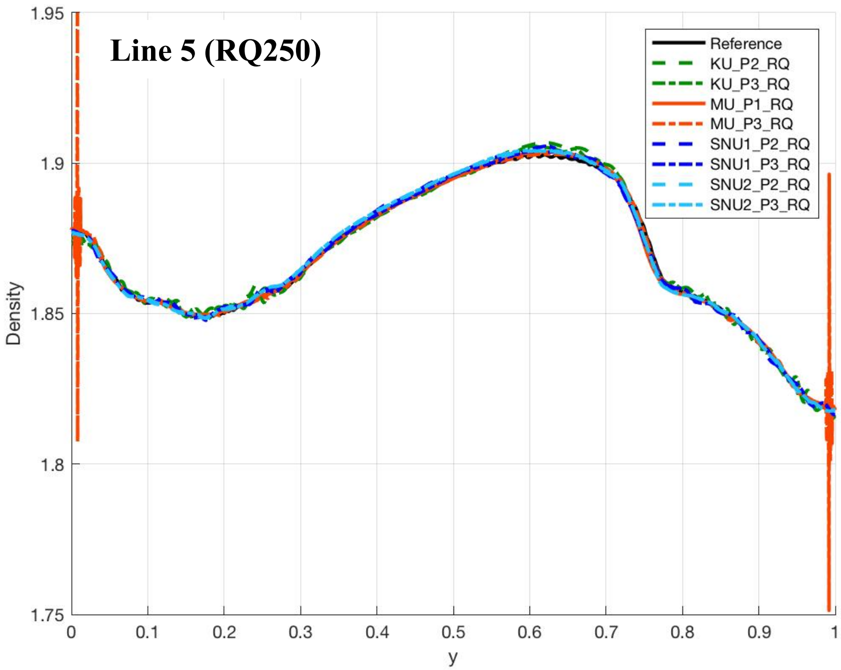

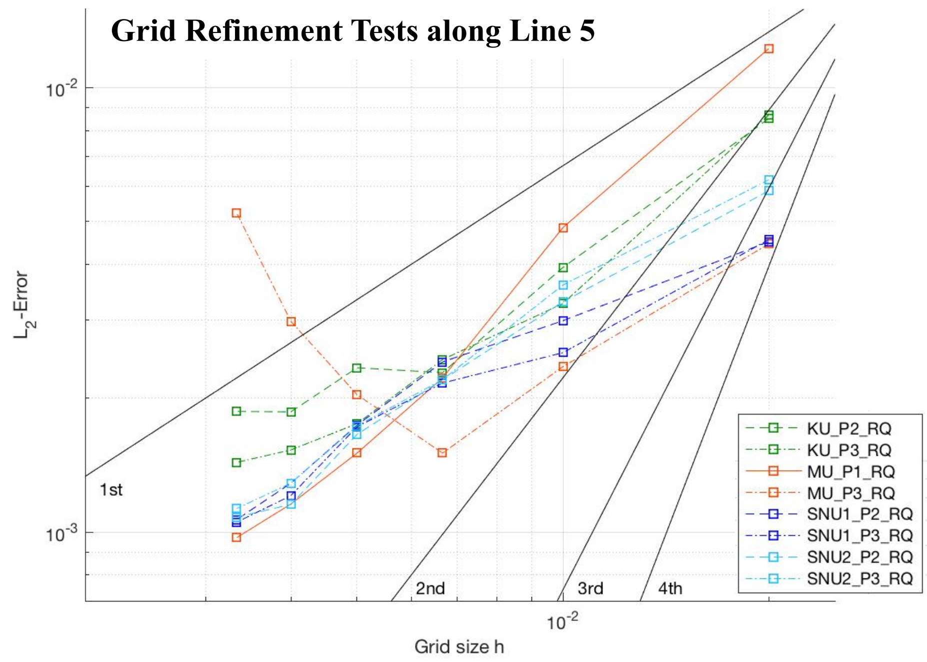

Order-of-Accuracy Degradation

- **Factors affecting order-of-accuracy degradation**

Non-smooth region ⊃ Shock ⊃ Shock inside cells ⊃ Non-aligned shock

- **Additional test problems**
  - **Composite vortex is considered for all tests.**

Test Problem	Non-smooth region	Shock	Shock inside cells	Non-aligned shock
Vortex Transport (Baseline)	O	X	X	X
Vortex behind Stationary Shock	O	O	X	X
Vortex behind Stationary Shock inside a Cell	O	O	O	X
Vortex behind Non-aligned Stationary Shock	O	O	O	O

Order-of-Accuracy Degradation

- **Vortex transport (Baseline)**
  - **Non-smooth composite vortex in CI2.**
  - **Computational conditions**
    - Computational domain $\Omega = [0, 2]\times[0, 1]$
    - A strong vortex with $M_v = 0.9$ is initially centered at $(x_c,\ y_c) = (0.75,\ 0.5)$.
    - Freestream is set to downstream conditions of CI2 Problem.
    - Target time $t = 0.7$
  - **Test cases**
    - DG-$P2$ ad -$P3$ with no limiter, hMLP and hMLP_BD
    - Test meshes: RQ50, RQ100, RQ200, RQ300

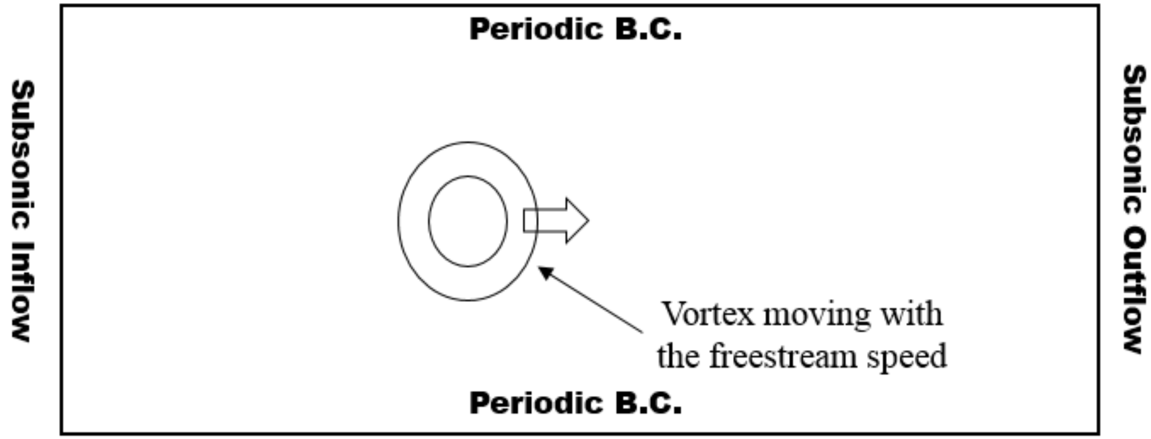

Schematic View of Vortex Transport Problem

Order-of-Accuracy Degradation

- **Vortex behind stationary shock**
  - Stationary shock is exactly aligned with a cell interface.
  - Baseline + Stationary shock ($M_s = 1.5$) at $x = 0.5$
- **Vortex behind stationary shock inside a cell**
  - Stationary shock is located inside a cell.
  - Baseline + Stationary shock ($M_s = 1.5$) at $x = 0.5 + \varepsilon$ where $\varepsilon = h/2$
- **Vortex behind non-aligned stationary shock**
  - Stationary shock is located along the regularly perturbed meshes.
  - Baseline + Stationary shock ($M_s = 1.5$) at $x = 0.5$ + Regularly perturbed mesh at stationary shock location

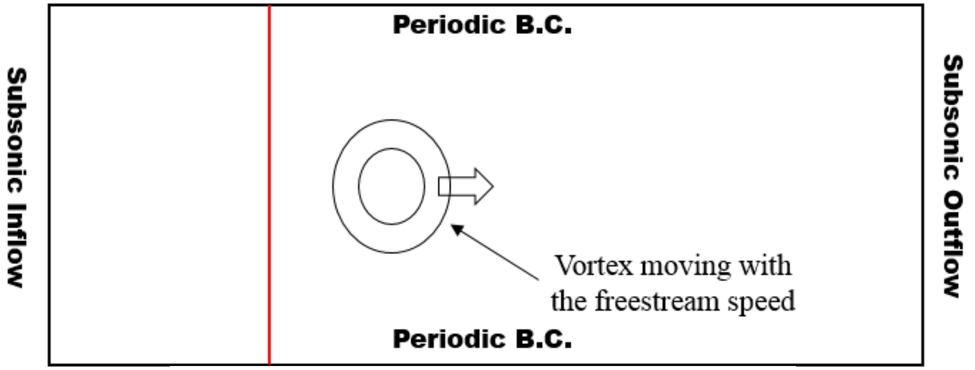

Schematic View of Vortex-Shock Problems

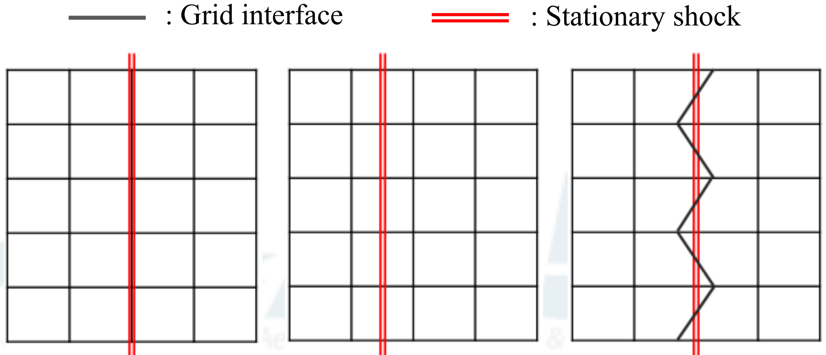

Aligned Shock | Shock inside a Cell | Regularly Perturbed Mesh

Order-of-Accuracy Degradation

- **Effects of each factor**

Test Problem	DG-$P2$ hMLP	DG-$P2$ hMLP_BD	DG-$P2$ no limiter	DG-$P3$ hMLP	DG-$P3$ hMLP_BD	DG-$P3$ no limiter
Vortex Transport (Baseline)	**1.954**	**1.785**	**1.950**	**1.883**	**1.785**	**2.155**
Vortex behind Stationary Shock	1.980 **(+0.026)**	1.793 **(+0.008)**	-	1.821 **(-0.062)**	1.790 **(+0.005)**	-
Vortex behind Stationary Shock inside a Cell	1.798 **(-0.156)**	1.398 **(-0.387)**	-	1.864 **(-0.019)**	1.167 **(-0.618)**	-
Vortex behind Non-aligned Stationary Shock	0.966 **(-0.988)**	1.527 **(-0.258)**	-	0.804 **(-1.079)**	1.576 **(-0.209)**	-

( ) : Order-of-accuracy degradation with respect to the baseline test

- **In the baseline test, formal order-of-accuracy is not preserved even when the limiter is not used. Projection error seems to be the main cause of the degradation.**
- **If the shock is located at the interface of meshes, it does not affect the order-of-accuracy.**
- **If the shock is located inside a cell or not aligned with meshes, non-physical oscillations generated by the shock negatively affect the order-of-accuracy.**

Order-of-Accuracy Degradation

- **Projection error**
  - **Projection error occurs when the exact initial profile is projected onto *Pn*-polynomial space.**
  - **Grid refinement test is conducted to measure projection error of baseline vortex problem.**
  - **Due to projection error, the formal order-of-accuracy could not be achieved.**
  - **Computed order-of-accuracy**
    - *x*-Momentum (C^0-continuous profile): DG-*P2*: 1.568, DG-*P3*: 1.520
    - Density (C^1-continuous profile): DG-*P2*: 2.390, DG-*P3*: 2.549

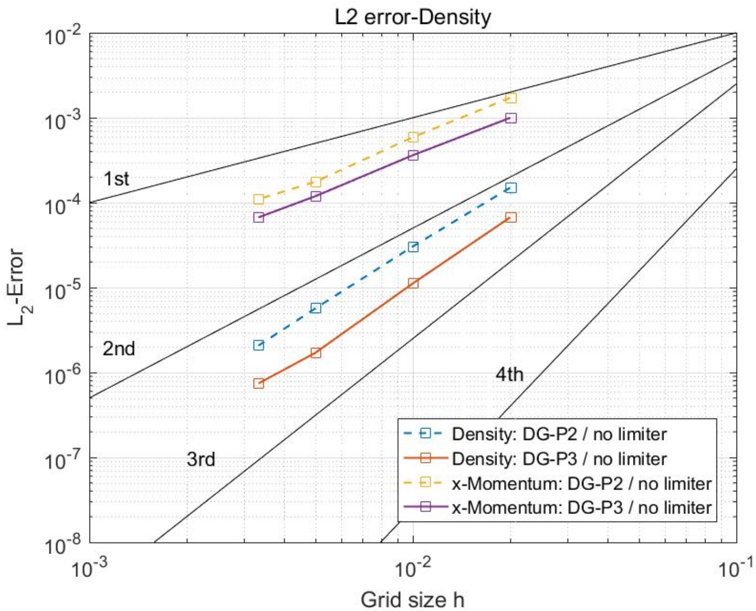

Grid Refinement Test of Projection Error

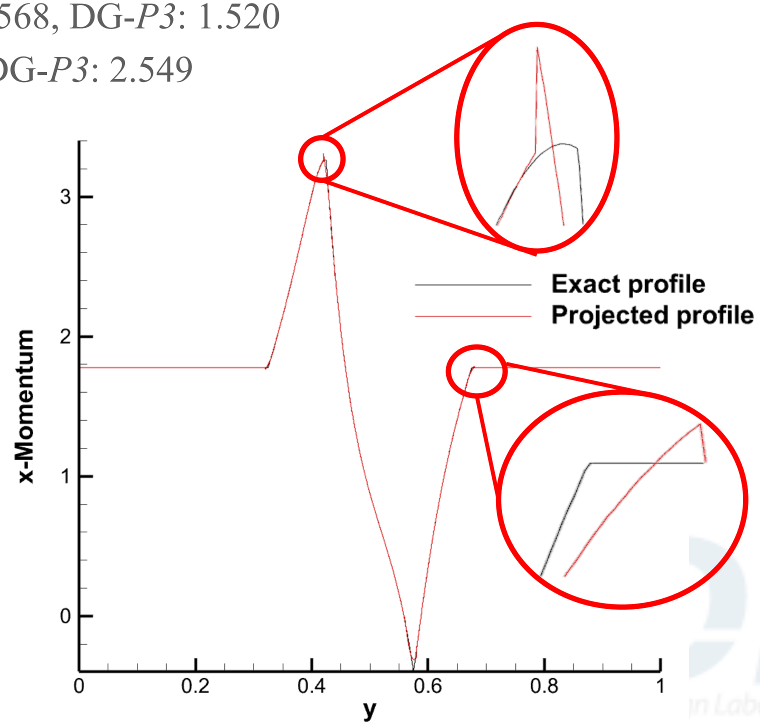

***x*-Momentum Profile along a Vertical Line Passing Vortex Core at Initial Condition**

Open Discussion

Observations

- **High-order methods can resolve complex flow structures of shock-vortex interaction with less DOFs than finite volume methods, but yield some unwanted numerical artifacts across shock and post-shock region.**

- **In highly non-linear problem with non-smooth profile, we have degradation in order-of-accuracy.**
  - **All schemes shows approximately show ~ 2^{nd} ~ -order accuracy.**

- **Several factors affecting the formal order-of-accuracy in high-order methods.**
  - **Projection error of a non-smooth initial profile**
  - **Non-physical oscillations (numerical flux, limiting strategy/amount of diffusion, shock-alignment & mesh distribution, etc)**

- **Further studies are necessary to improve accuracy, efficiency and robustness of high-order methods for unsteady compressible flows.**

Appendix

- **Reliability of reference solution**
  - **In order to observe the behavior of order test results with respect to the reference solution, 1-D smooth problem is examined.**
  - **Problem description**
    - Non-dimensional 1-D Euler equations with EOS for ideal gas
    - Initial condition: $[\rho, u, p] = [1 + 0.2\sin(2\pi x), 1,1]$
    - Computational domain: $\Omega = [0,1]$
    - Target time: $t = 1$
    - Grid sizes for DG method: $h = \frac{1}{15}, \frac{1}{30}, \frac{1}{60}, \frac{1}{90}$

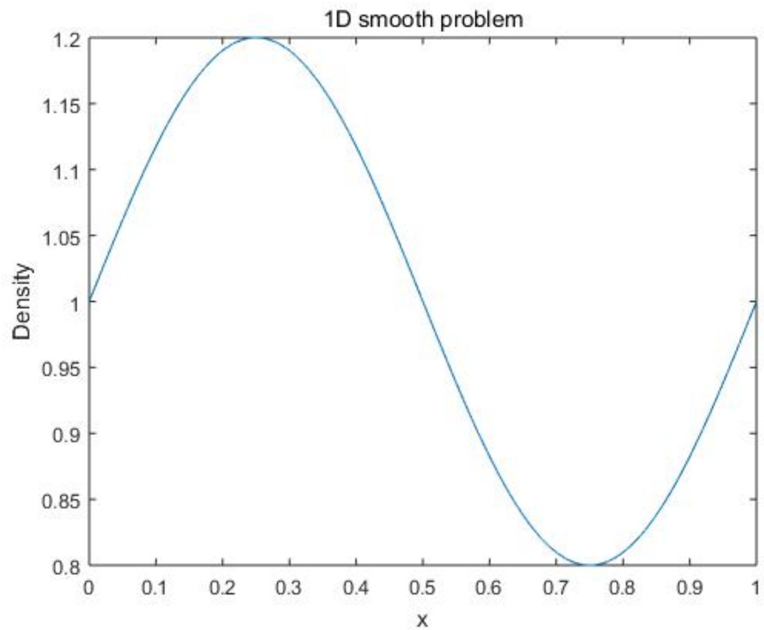

Density Profile

Appendix. Reference Solution

- **Reliability of reference solution (*Cont'*)**
  - **Error of the DG solution is measured with the reference solution, which is computed by FVM with fine meshes.**
  - **Judging from the observation in the 1-D smooth problem, if the reference solution is obtained on sufficiently fine meshes, the order-of-accuracy is correctly behaved, otherwise the error is saturated at some point.**

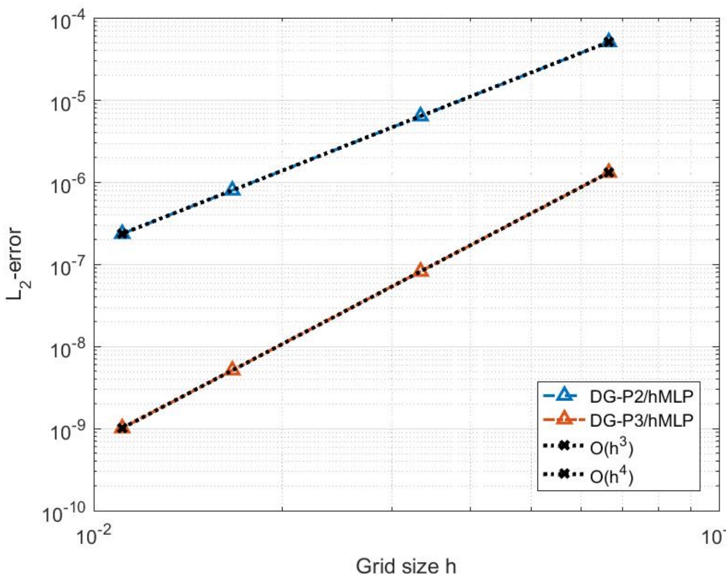

(a) FVM results from $h = \frac{1}{1{,}000{,}000}$

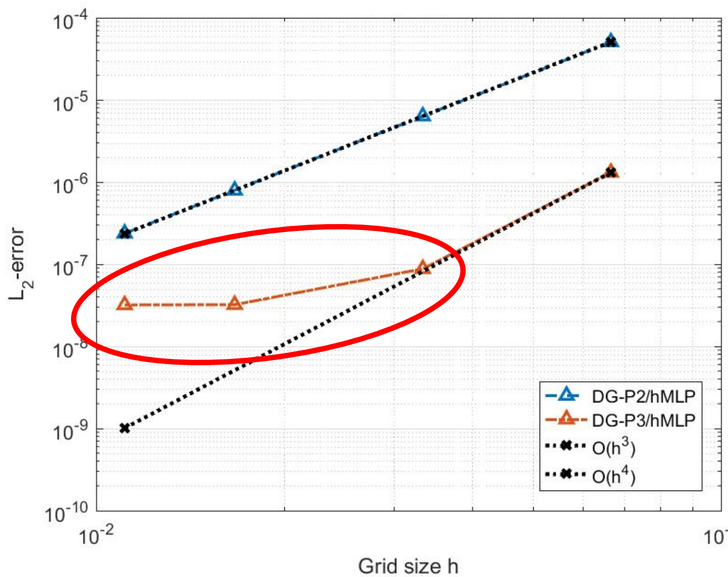

(b) FVM results from $h = \frac{1}{10{,}000}$

L2 Error Measured with the Reference Solution

Appendix. Results (Line 2 & 4)

- **Line 2: Similar shock structure shown in Line 1**
  - **Solution behavior around the shock is similar to Line 1.**
  - **Non-monotonicity of shock is shown more clearly in Line 2.**
- **Line 4: Similar vortical structure shown in Line 1**
  - **Solution behavior around vortex core is similar to Line 1.**
  - **Difference in location and depth of the vortex core is more apparent in Line 4.**

Line 2 (RQ250)

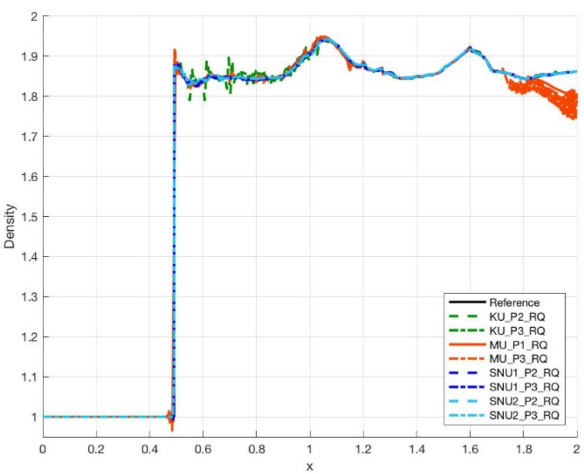

Line 2 (Shock Close-up)

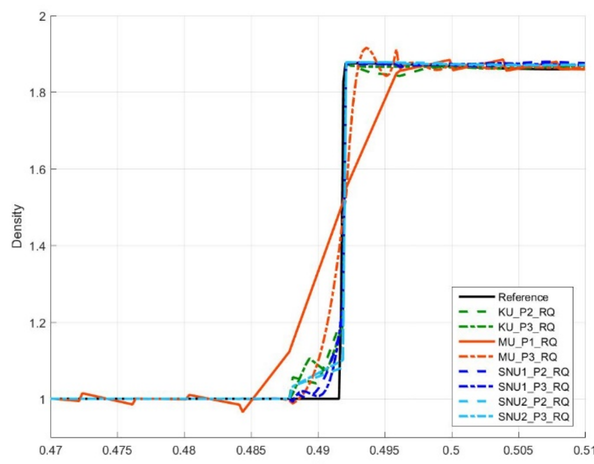

Line 4 (RQ250)